Journal of Alloys and Compounds 490 (2010) 331–335

Contents lists available at ScienceDirect

Journal of Alloys and Compounds

journal homepage: www.elsevier.com/locate/jallcom

Synthesis and formation mechanism of urchin-like nano/micro-hybrid α-MnO_2

Yong Chen[a,b,*], Yuzhen Hong[a,b], Yanping Ma[a,b], Jianbao Li[a,b]

[a] *Ministry of Education Key Laboratory of Application Technology of Hainan Superior Resources Chemical Materials, Haikou 570228, PR China*
[b] *Hainan Provincial Key Laboratory of Research on Utilization of Si-Zr-Ti Resources, Hainan University, Haikou 570228, PR China*

ARTICLE INFO

Article history:
Received 11 June 2009
Received in revised form 1 October 2009
Accepted 1 October 2009
Available online 6 October 2009

Keywords:
X-ray diffraction
Chemical synthesis
Nanostructures

ABSTRACT

Urchin-like nano/micro-hybrid α-MnO_2 balls were prepared through the hydrothermal reaction of H_2SO_4 and $KMnO_4$ without the use of templates, surfactants or other additives. The products were characterized by scanning electron microscopy (SEM), transmission electron microscopy (TEM), energy dispersive spectroscopy and X-ray diffraction (XRD). It indicates that the urchin-like α-MnO_2 is composed of single crystalline α-MnO_2 nanorods. The formation mechanism of urchin-shaped α-MnO_2 was proposed and explained in detail on the basis of the time-dependent designed experiments combined with XRD analysis and TEM observations of the intermediates during the formation process.

1. Introduction

As a kind of important metal oxide, manganese dioxide is one of the most attractive inorganic materials because of its physical and chemical properties and wide applications in catalysis [1], molecular-sieves [2], ion exchange, biosensor, and especially energy storage, such as electrode materials in Li/MnO_2 batteries [3,4] and supercapacitors [5,6] due to its energy compatibility with a reversible lithium electrochemical system, environmental friendliness and low cost. It is well-known that manganese dioxide can exist in different crystal structures, including α-, β-, γ-, ε-, η-, δ-, and λ-MnO_2, etc., when the basic structural unit [MnO_6] is linked in different manners. According to different [MnO_6] octahedron links, the MnO_2 structures can be divided into three categories: the chain-like tunnel structure such as α-, β-, and γ-crystalline form; the sheet or layered structure such as δ-type; and the third category that is composed of three-dimensional structures such as λ-MnO_2. The different crystalline structures of manganese dioxide exhibit different properties and life cycles [7]. In addition to the crystal structure, the size and morphologies of MnO_2 particles also play a key role in determining the properties for practical applications. In this regard, many efforts have been made to prepare nanocrystalline MnO_2 with different structures and shapes. Up to now, various nanostructures of MnO_2, such as nanoparticles, nanorods, belts, wires, tubes, fibers, urchins/orchids, mesoporous and branched structures, have been synthesized by different methods. Most 1D structural MnO_2 are prepared by the hydrothermal method via deposition–precipitation at high reaction temperature and pressure [8–11]. In particular, MnO_2 with the new shape has attracted interest from researchers owing to its potential applications and novel physical and chemical properties. Generally, urchin-like α-MnO_2 is synthesized with the addition of a template, surfactant, or any other additives [12–15]. In previous work, single-crystal α-MnO_2 nanorods were prepared in H_2SO_4 solution by adding $KMnO_4$ at the temperatures of 70–95 °C [16]. Interestingly, it was found that α-MnO_2 nanorods can aggregate together, forming a ball-like shape. However, knowledge on its growth mechanism is still quite limited. In fact, how these nanorods aggregated without the templates or other additives remains to be examined.

In this work, we introduced a simple approach to synthesize an urchin-like structure α-MnO_2 which is composed of a single-crystal α-MnO_2 nanorod using a hydrothermal reaction at low temperature without expensive raw materials or equipments. Compared to other methods, the current one did not use any templates, surfactants, or additives. In addition, the short reaction time of about 0.5 h and the low reaction temperature are its distinct advantages. Since α-MnO_2 has wider application in Li-ion batteries and supercapacitors, the urchin-like α-MnO_2 particles developed by the current method may be useful for energy storage [11]. This is one relevant topic that can be explored in the future. In addition, the urchin-like α-MnO_2 particle formed may provide new opportunities for fundamental studies to elucidate the growth mechanisms of the new shape nanomaterials without use of templates.

2. Experimental

All the chemicals used in this experiment were of analytical grade and were used without further purification. In a typical procedure, $KMnO_4$ powder was added to

* Corresponding author at: Ministry of Education Key Laboratory of Application Technology of Hainan Superior Resources Chemical Materials, Renming Road 58, Haikou 570228, PR China. Tel.: +86 898 66279122.
E-mail address: ychen2002@163.com (Y. Chen).

0925-8388/$ – see front matter © 2009 Elsevier B.V. All rights reserved.
doi:10.1016/j.jallcom.2009.10.004

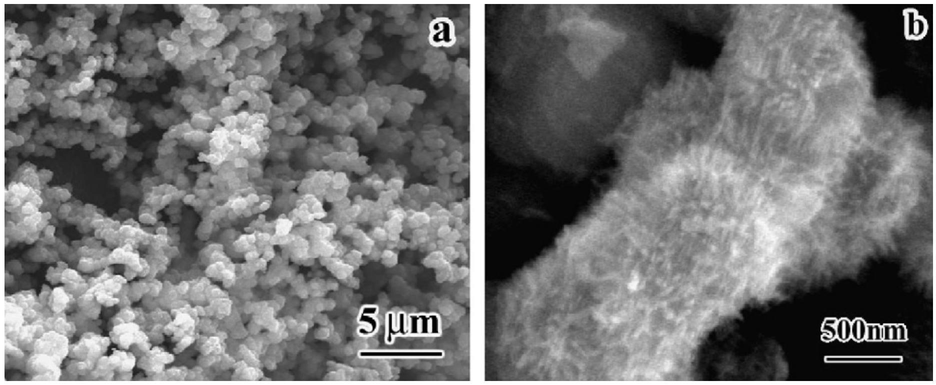

Fig. 1. SEM images of the urchin-like α-MnO_2 (a) and their enlarged view (b).

the sulphuric acid aqueous solution at 55 °C with strong magnetic stirring in a digital water bath then it was heated up to 85 °C. Precipitates were immediately produced after the addition of $KMnO_4$ powder, and the solution color changed during the reaction. The reaction course was monitored through the color change from purple to brown. The whole reaction lasted for about 0.5 h. After reaction the system was cooled to room temperature. The obtained products were washed thoroughly with deionized water in order to remove the possible remaining ions, and then were dried at 80 °C for 48 h.

The chemical composition of the as-synthesized products was analyzed by energy dispersive spectroscopy (EDS, Oxford unit) at an acceleration voltage of 20 kV in transmission electron microscopy (TEM, JEOL 2010), and their crystal structures were analyzed by X-ray diffraction (XRD, Bruker D8 Advance) with CuKα radiation. The morphologies of the samples obtained were observed with TEM, high-resolution transmission electron microscopy (HRTEM) at an acceleration voltage of 200 kV, and scanning electron microscopy (SEM, JSM-6301F). TEM specimens were prepared by dispersing the as-prepared samples in alcohol, then dipping a TEM sample grid into the dispersion. The specific surface area was measured by nitrogen cryo-adsorption apparatus (Micromeritics, ASAP 2010) at 77 K. Powder products were outgassed at 200 °C under 10^{-4} Pa for 9 h in vacuum before the measurement.

3. Results and discussion

It is interesting to find that all the products observed by SEM are uniformly spherical with a mean diameter of 1 μm (as shown in Fig. 1a). The products are composed of tiny fibers (shown in Fig. 1b). In addition, the shapes are spherical or elliptical.

To further investigate their microstructures, the spherical particles were examined by TEM. Uniform α-MnO_2 nanorods having sharp tips with a mean diameter of 10 nm and a length of 200 nm were aggregated to an urchin-like ball as shown in Fig. 2a. The enlarged view can be seen in the inset of Fig. 2a. It shows the typical HRTEM image of a single nanorod as shown in Fig. 2b. The clear lattice fringes illustrate that the nanorod is a single crystal, and the inter-layer space is about 0.7 nm, corresponding to the [1 1 0] plane of α-MnO_2. Likewise, a typical tip of a nanorod can be clearly seen to be gradually sharpened (Fig. 2c). This is probably because of the reduced concentration of the $KMnO_4$ towards the end of the reaction.

The chemical compositions of the as-prepared product were examined by using EDS in TEM. The result (Fig. 3) shows that the products are composed of elements Mn, O, and a small amount of K. The peak of element Cu was caused by the Cu micro-grid which was used for supporting the samples. The atomic ratio of the component elements is listed in Table 1. As shown, the atomic ratio of element O to Mn is 2.14, a little bigger than 2. The surface Cu of the

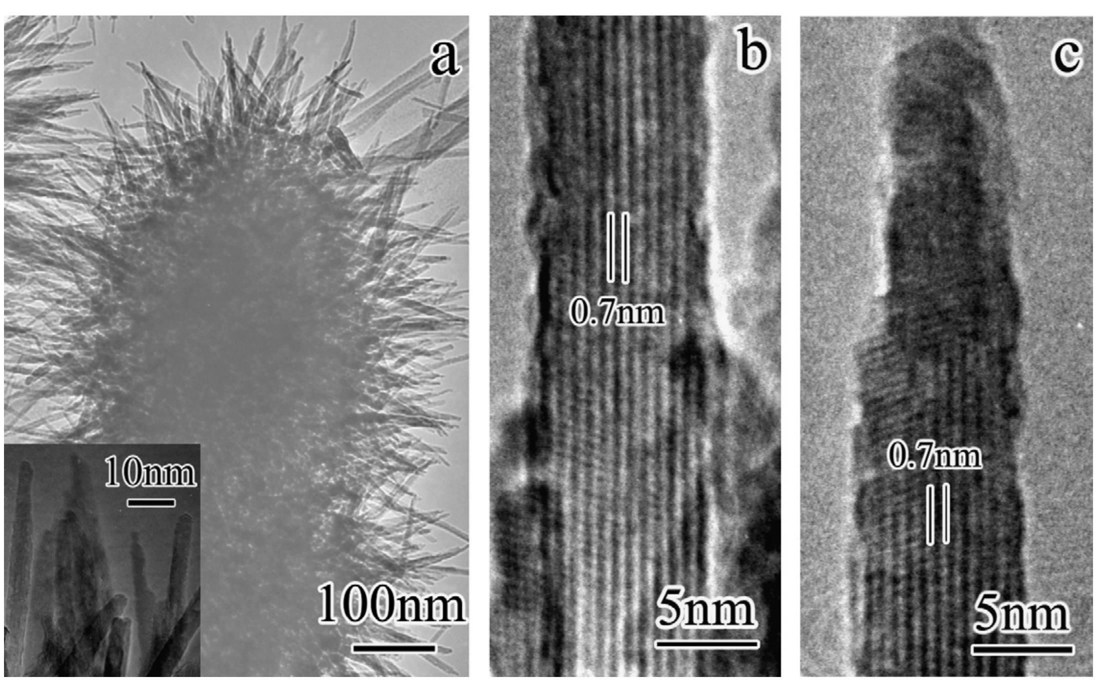

Fig. 2. TEM images of the α-MnO_2 nanorods with a diameter of 10 nm (a) and their enlarged view (inset), their HRTEM image corresponding to [1 1 0] (b) and the tip of the nanorod (c).

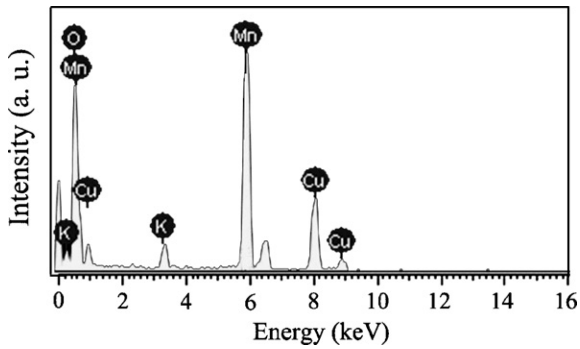

Fig. 3. EDS analysis of the as-prepared α-MnO_2 products.

Table 1
EDS analysis of the as-prepared α-MnO_2 products.

Element	Weight %	Atomic %
O	29.43	59.34
K	3.40	2.81
Mn	47.29	27.77
Cu	19.87	10.09
Total	100.00	100.00

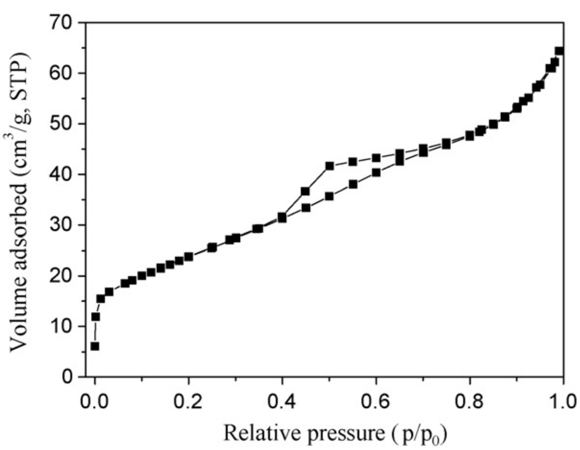

Fig. 4. The cryo-nitrogen adsorption isotherm of the urchin-like α-MnO_2 balls at 77 K.

micro-grid, which was oxidized, can account for this observation.

Fig. 4 is the nitrogen adsorption and desorption isotherms of urchin-like α-MnO_2 balls. The samples were found to possess a high BET specific surface area up to 85.9 m^2/g. A gradual uptake of N_2 is observed at the medium P/P_0, which indicates that the urchin-like α-MnO_2 has large external surface area due to their small diameter.

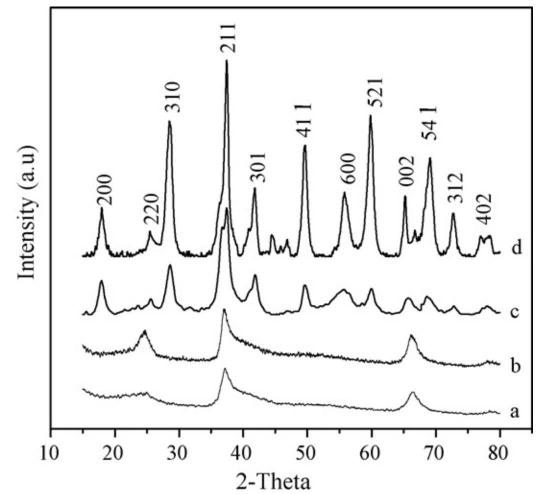

Fig. 5. XRD pattern of the as-prepared α-MnO_2 sample: (a) 55 °C; (b) 65 °C; (c) 75 °C; (d) 85 °C.

The appearance of the clear hysteresis of N_2 isotherms suggests that the urchin-like α-MnO_2 possess some mesopores originated from the aggregated α-MnO_2 nanorods.

To investigate the as-synthesized products' crystal structures, XRD was employed. The XRD pattern obtained is shown in Fig. 5d. All the diffraction peaks can be perfectly indexed to the tetragonal α-MnO_2 single crystal structure [space group: $I4/m$ (87)] with lattice constants of a = 9.784 Å and c = 2.863 Å, indicating the high purity and crystallinity of the obtained product.

The α-MnO_2 crystal structure is composed of an [MnO_6] octahedron, as shown in Fig. 6. α-MnO_2 is constructed from the double chains of [MnO_6] octahedral forming 2 × 2 tunnels. The Mn atoms located at the octahedral center, the six oxygen atoms located in the octahedral angle, and the [MnO_6] octahedral edge were connected to single-stranded or double-stranded chains. The chains were found on top of the tunnel structure, which formed the gap. It is known that α-MnO_2 has a tunnel structure, generally with some large cations (such as K^+, Ba^{2+}, Pb^{2+} or NH^+) embedded in its tunnel cavity [17,18] to stabilize its structure. Thus, the small amount of K (approximately 2.81%) detected by EDS (in Fig. 3 and Table 1) located within the tunnel of α-MnO_2 was possibly introduced by $KMnO_4$ in the reaction course.

From previous literatures, the specially shaped materials are generally prepared in the presence of a template or other ions. The urchin-like α-MnO_2 in our experiment was formed without any templates or surfactants. To investigate the formation process of the urchin-shaped structures, we collected some of their intermediates during the formation process and observed them by SEM. As shown in Fig. 7a, the intermediates obtained under 55 °C

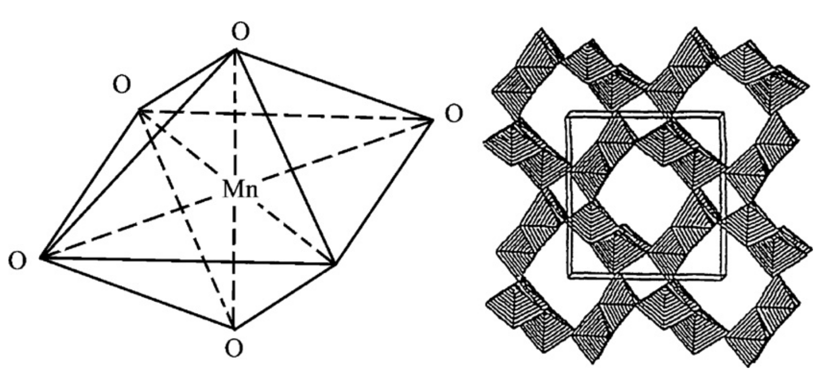

Fig. 6. [MnO_6] octahedral structure and α-MnO_2 structure.

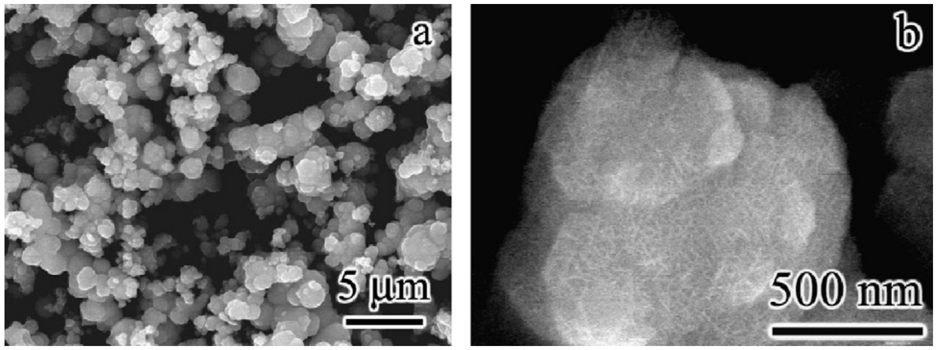

Fig. 7. SEM images of the sample obtained at 55 °C (a) and their enlarged view (b).

hydrothermal conditions for 10 min, which underwent fast cooling and washing by deionized water and drying at temperature of 110 °C, are microspheres with diameters of 1 μm; they consist of small nanorods. These are shown in an enlarged SEM view in Fig. 7b and TEM view in Fig. 8a. Due to the lower initial temperature (55 °C) at the original time, the reaction rate of H_2SO_4 and $KMnO_4$ was slow, which led to the formation of a bulk product. From SEM, the products were also shown as well-defined ball-like particles with diameters of 1 μm, and a lot of tiny rods were inserted into the film.

It shows the TEM image of the intermediates (in Fig. 8b) obtained under 65 °C hydrothermal conditions for 10 min, followed by fast cooling and washing. The image indicates that many nanorods are epitaxially grown from nanoparticles on the surface of the microspheres.

Upon a further increase of the reaction temperature to 75 °C under hydrothermal conditions for 10 min, the morphology of the obtained MnO_2 turned into a follower-shape and the nanorods in the follower-shaped structure were formed and became long as shown in Fig. 9a. In the enlarged HRTEM image of a single nanorod, the clear lattice fringes illustrate that the nanorod is a single crystal, of which inter-layer space is about 0.7 nm, corresponding to the [1 1 0] plane of α-MnO_2. Therefore, it is reasonable to deduce that these rods grew longer with the increase of reaction time. Compared with the intermediates, the final products obtained under the 85 °C hydrothermal conditions show that the microspheres transformed into a sea urchin-shaped α-MnO_2. At the end of the reaction, due to the depletion of $KMnO_4$, the sharp tip of the rod grew to nanorods with a length of 200 nm. Thus, the urchin-like nano/micro-hybrid α-MnO_2 was formed. This suggests that the crystal shape and size of the products obtained strongly depend on the reaction temperature.

It is shown by further XRD characterization that the crystal structure of the samples obtained at temperature of 55 °C and 65 °C is that of δ-MnO_2 (Fig. 5a and b). However, its crystal structure was transformed to that of α-MnO_2 with an increase temperature to 75 °C (Fig. 5c). Likewise, the diffraction peaks are wider while their intensities are lower, suggesting poor crystallinity. Fig. 5d shows the diffraction peaks of the final products obtained under the 85 °C hydrothermal conditions. Note that all the diffraction peaks can be perfectly indexed to the tetragonal α-MnO_2 single crystal structure. This indicates that the samples obtained at 85 °C are well-defined α-MnO_2 and correspond to a complete crystal structure in accordance with the HRTEM observations (Fig. 2b). It was found that only δ-MnO_2 microspheres were obtained when the sulphuric acid concentration was below 2.5 mol/L. While above this concentration, urchin-shaped α-MnO_2 can be obtained, which was also affected by the reaction temperature generally at or above 85 °C. The length of nanorods was increased with the increasing reaction time.

The existence of inter-layer K^+ and water molecules in the layered structure of δ-MnO_2 is the basis for keeping structural stability. Thermo-gravimetric analysis showed that the bound water of δ-MnO_2 was about 20%, while it was only 5% in α-MnO_2. This further indicates that the crystal structure of MnO_2 has a close relation with bound water. δ-MnO_2 contains more bound water and inter-layer K^+ due to its large layer interval; in contrast, the amount of bound water in α-MnO_2 tunnel structure was much lower than that in δ-

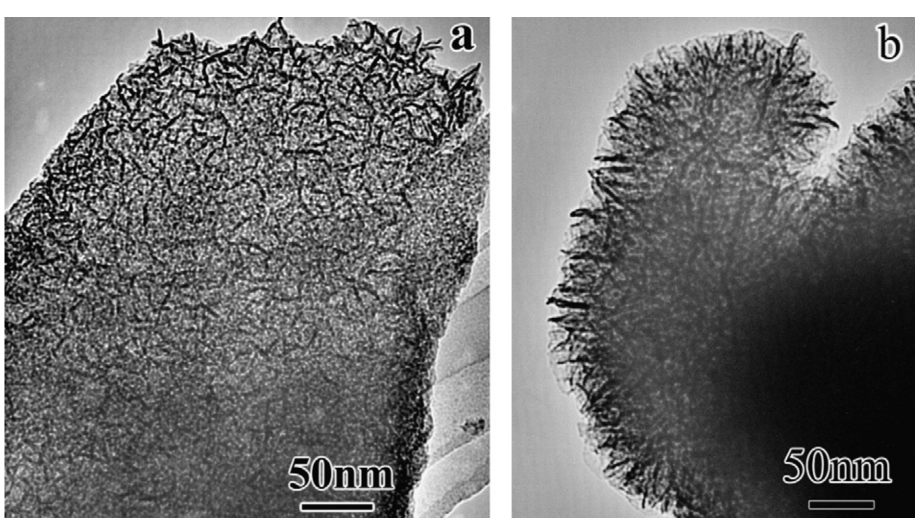

Fig. 8. TEM images of the sample obtained at 55 °C (a) and 65 °C (b).

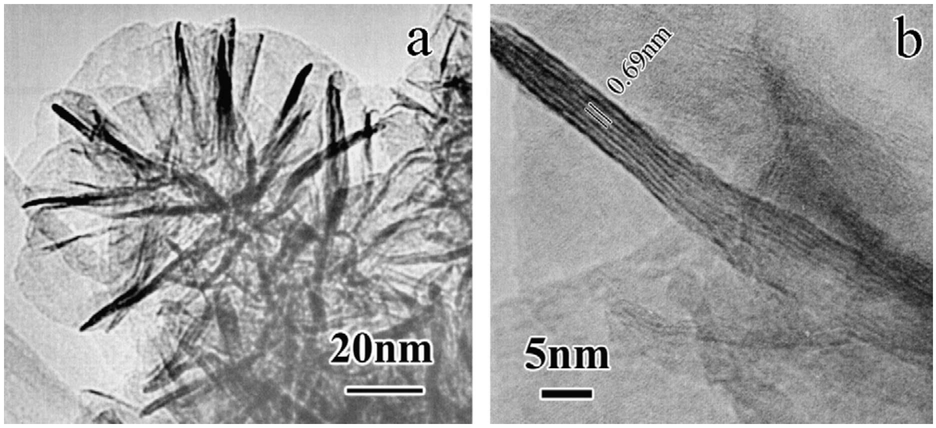

Fig. 9. TEM images of the sample obtained at 75 °C (a) and their enlarged view (b).

MnO_2. According to the above results, the generation of α-MnO_2 at higher sulphuric acid concentration and reaction temperature indicates that acid has great effect on the decrease of bound water in crystal structure. The increase of sulphuric acid concentration weakened the bonding capability between K^+ and water molecules and demolished their bond, and the increased temperature further promoted the demolishing capability of acid; due to the large layer interval in the layered structure of δ-MnO_2, destroyed inter-layer hydrated ions of K^+ may lead to the layered structure to collapse, thus forming α-MnO_2 tunnel structure. With further increase in temperature, the α-MnO_2 nanorods grew out from the sphere, leading to the formation of sea urchin-like structures.

4. Conclusions

In summary, urchin-like α-MnO_2 microspheres composed of α-MnO_2 nanorods with small diameters have been successfully synthesized via a simple hydrothermal process with $KMnO_4$ in H_2SO_4 solution. The experimental results showed that the crystal structure, shape and size of the products obtained depend strongly on both the H_2SO_4 concentration and reaction temperature. Through the structural analysis and morphological observation of the intermediate product obtained at different time during the formation process, it was found that the δ-MnO_2 ball-shaped particles were synthesized at a low temperature at the initial time. With increasing reaction temperature, a lot of α-MnO_2 nanorods were formed and gradually grew out of the layered δ-MnO_2 structure, consequently forming the urchin-like α-MnO_2 consisted of radically grown single crystalline α-MnO_2 nanorods with diameters of 10 nm and length of 200 nm.

Acknowledgements

This work was supported by the National Natural Science Foundation of China (No. 50762003), the Natural Science Foundation of Hainan Province (No. 807009), and the Education Department of Hainan Province (Hjkj2008-03).

References

[1] N. Sui, Y. Duan, X. Jiao, D. Chen, J. Phys. Chem. C 113 (2009) 8560–8565.
[2] J. Yuan, W. Li, S. Gomez, S. Suib, J. Am. Chem. Soc. 127 (2005) 14184–14185.
[3] F. Jiao, P.G. Bruce, Adv. Mater. 19 (2007) 657–660.
[4] M. Minakshi, K. Nallathamby, D.R. Mitchell, J. Alloys Compd. 479 (2009) 87–90.
[5] W. Xiao, H. Xia, J. Fuh, L. Lu, J. Power Sources 193 (2009) 935–938.
[6] Y. Yang, E. Liu, L. Li, Z. Huang, H. Shen, X. Xiang, J. Alloys Compd. (2009), doi:10.1016/j.jallcom.2009.08.008.
[7] S. Devaraj, N. Munichandraiah, J. Phys. Chem. C 112 (2008) 4406–4417.
[8] X. Wang, Y.D. Li, J. Am. Chem. Soc. 124 (2002) 2880–2881.
[9] Z.Y. Yuan, Z. Zhang, G. Du, T.Z. Ren, B.L. Su, Chem. Phys. Lett. 378 (2003) 349–353.
[10] Y. Gao, Z. Wang, J. Wan, G. Zhou, Y. Qian, J. Cryst. Growth 279 (2005) 415–419.
[11] Z. Zhang, J. Mu, Solid State Commun. 141 (2007) 427–430.
[12] P. Yu, X. Zhang, D. Wang, L. Wang, Y. Ma, Cryst. Growth Des. 9 (2009) 528–533.
[13] X.C. Song, Y. Zhao, Y.F. Zheng, Cryst. Growth Des 7 (2007) 159–162.
[14] X. Li, W. Li, X. Chen, C. Shi, J. Cryst. Growth 297 (2006) 387–389.
[15] H. Wang, Z. Lu, D. Qian, S. Fang, J. Zhang, J. Alloys Compd. 466 (2008) 250–257.
[16] Y. Chen, C. Liu, F. Li, H.M. Cheng, J. Alloys Compd. 397 (2005) 282–285.
[17] N. Kijima, H. Yasuda, T. Sato, Y. Yoshimura, J. Solid State Chem. 159 (2001) 94–102.
[18] L. Li, Y. Pan, L. Chen, G. Li, J. Solid State Chem. 180 (2007) 2896–2904.